

# Characterization of the Optical and X-ray Properties of the Northwestern Wisps in the Crab Nebula

M.C. Weisskopf, N. Bucciantini, W. Idec, K. Nilsson, T. Schweizer, A.F. Tennant, R. Zanin

## Abstract (1)

We have studied the wisps to the northwest of the Crab pulsar as part of a multi-wavelength campaign in the visible and in X-rays. Optical observations were obtained using the Nordic Optical Telescope in La Palma and X-ray observations were made with the Chandra X-ray Observatory. The observing campaign took place from October 2010 until September 2012.

About once per year we observe wisps forming and peeling off from (or near) the region commonly associated with the termination shock of the pulsar wind. We find that the exact locations of the northwestern wisps in the optical and in X-rays are similar **but not coincident**, with X-ray wisps preferentially located closer to the pulsar. This suggests that the optical and X-ray wisps are not produced by the same particle distribution. It is also interesting to note that the optical and radio wisps are also separated from each other (Bietenholz et al. 2004).

Our measurements and their implications are interpreted in terms of a Doppler-boosted ring model that has its origin in MHD modeling. While the Doppler boosting factors inferred from the X-ray wisps are consistent with current MHD simulations of PWNe, the optical boosting factors are not, and typically **exceed values from MHD simulations by about a factor of 4**.

## Defining the radial and azimuthal distributions (2)

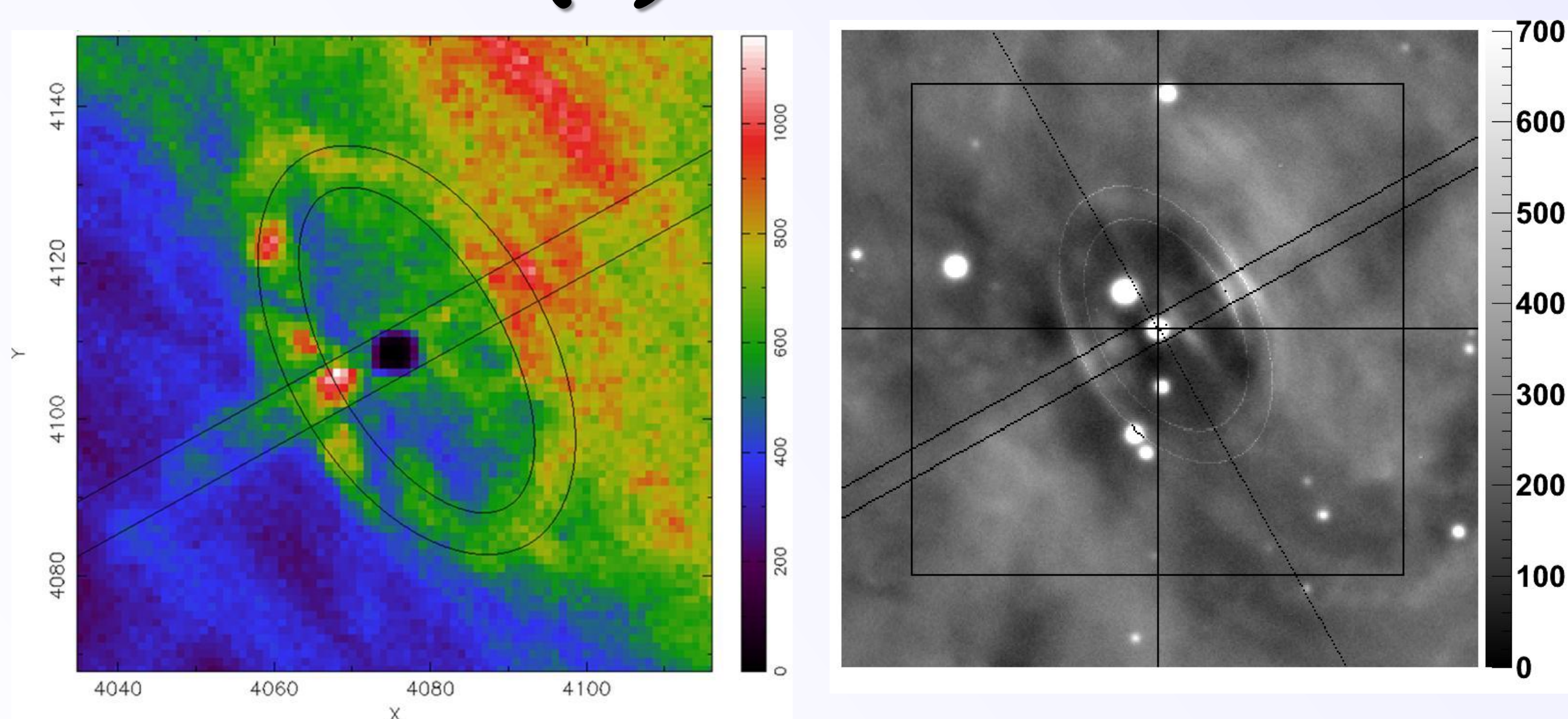


Figure 1. North is up and east is to the left in both images. Left: Chandra X-ray image of the Crab Nebula. The axes are ACIS pixels (0.492"/pixel). The two concentric ellipses bound the region selected for X-ray azimuthal distributions. The parallel lines bound the region used to determine radial profiles. The black feature with zero counts is the burned out (piled up) image of the pulsar. The color scale is counts per ACIS pixel (0.5-8 keV). Right: Corresponding optical image. The square covers a field of view of 50'' x 50''. The long, narrow rectangle outlines the region used to measure the radial profile. Two ellipses are shown that pass through the most prominent optical wisps at  $\sim 8.0''$  and  $\sim 10''$  NW of the pulsar.

## The X-ray radial distribution leads (closest to the pulsar) the optical (3)

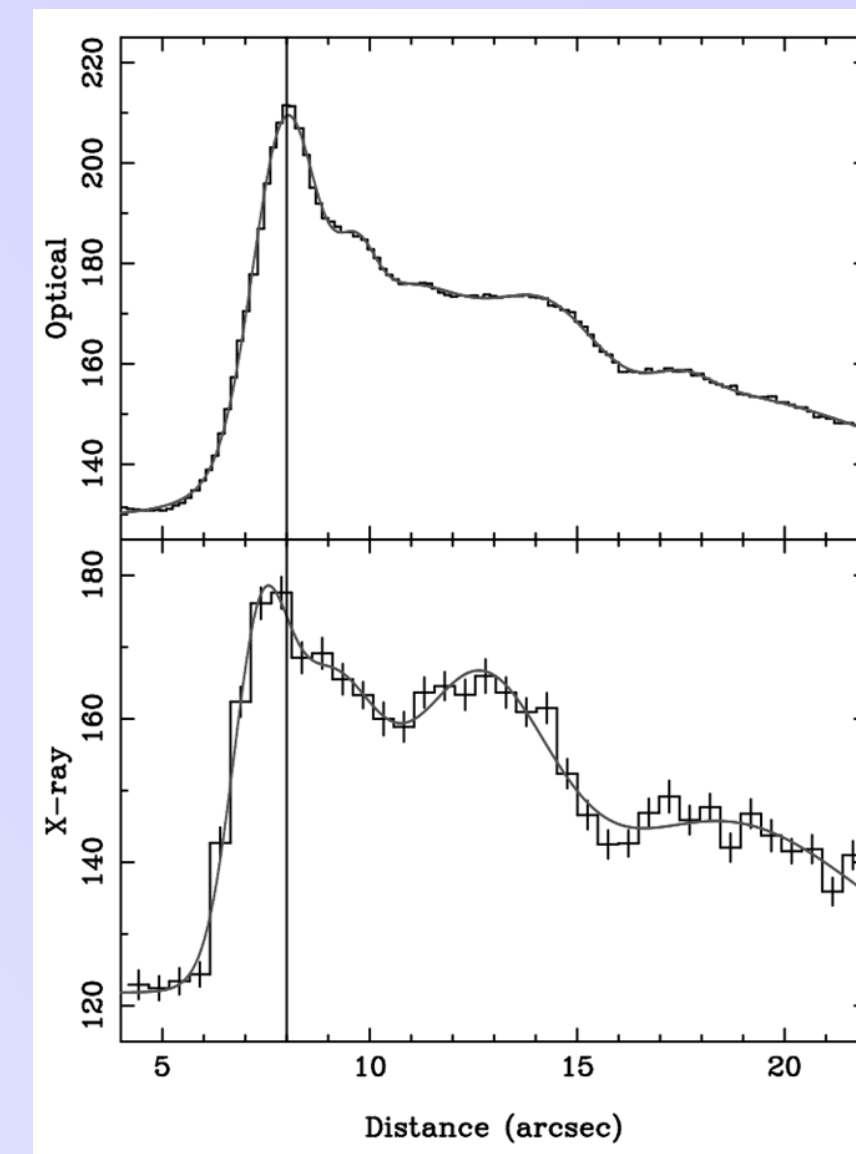


Figure 2. Upper panel: Two-year average radial profile for the optical observations ( $\mu\text{Jy}/\text{arcsec}^2$ ). Lower panel: Same as the upper panel, but now for the X-ray data. **Note the offset between the peak emissions.**

## Radial distributions to the NW of the pulsar as a function of time (4)

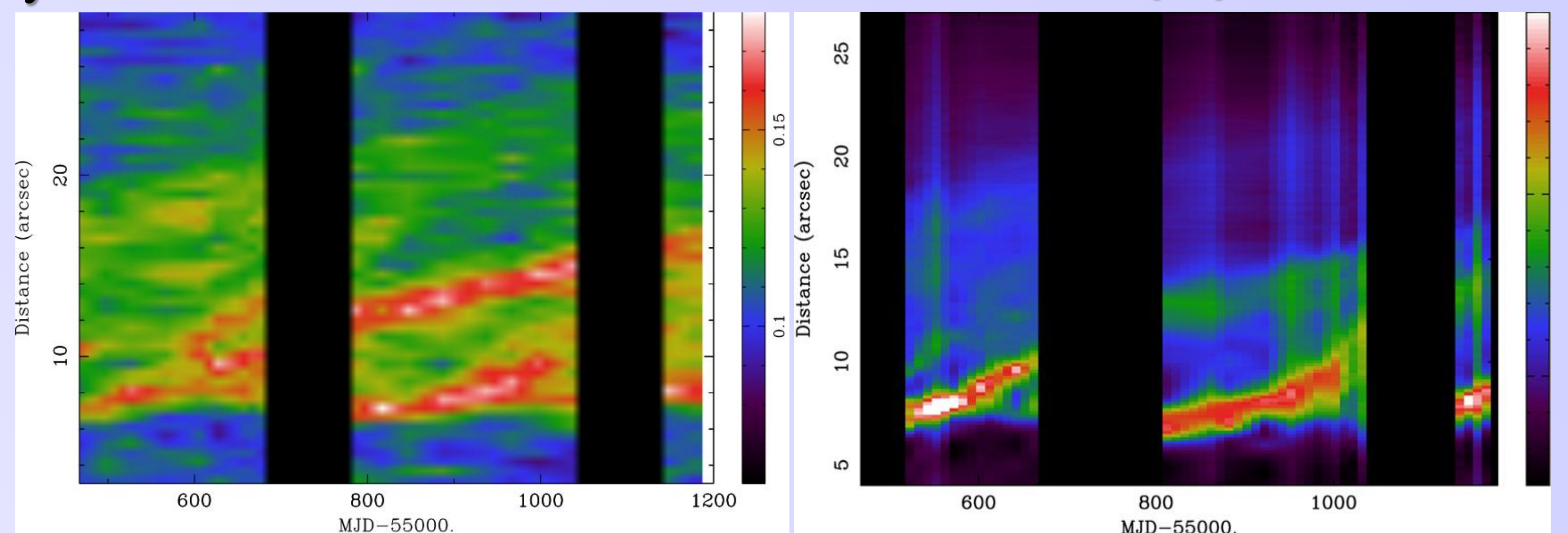


Figure 3. The two panels above compare the radial evolution of the optical (right panel) and X-ray (left panel) wisps as a function of time. Data were interpolated between observations but not across the large gaps imposed by sun constraints. The unit for the color scale are  $\mu\text{J}/\text{arcsec}^2$  for the right panel and counts for the left panel. [One might conclude that wisps form when the system is not observed! 😊] Apparent velocities @2kpc range from 0.1 to 0.4  $v/c$ .

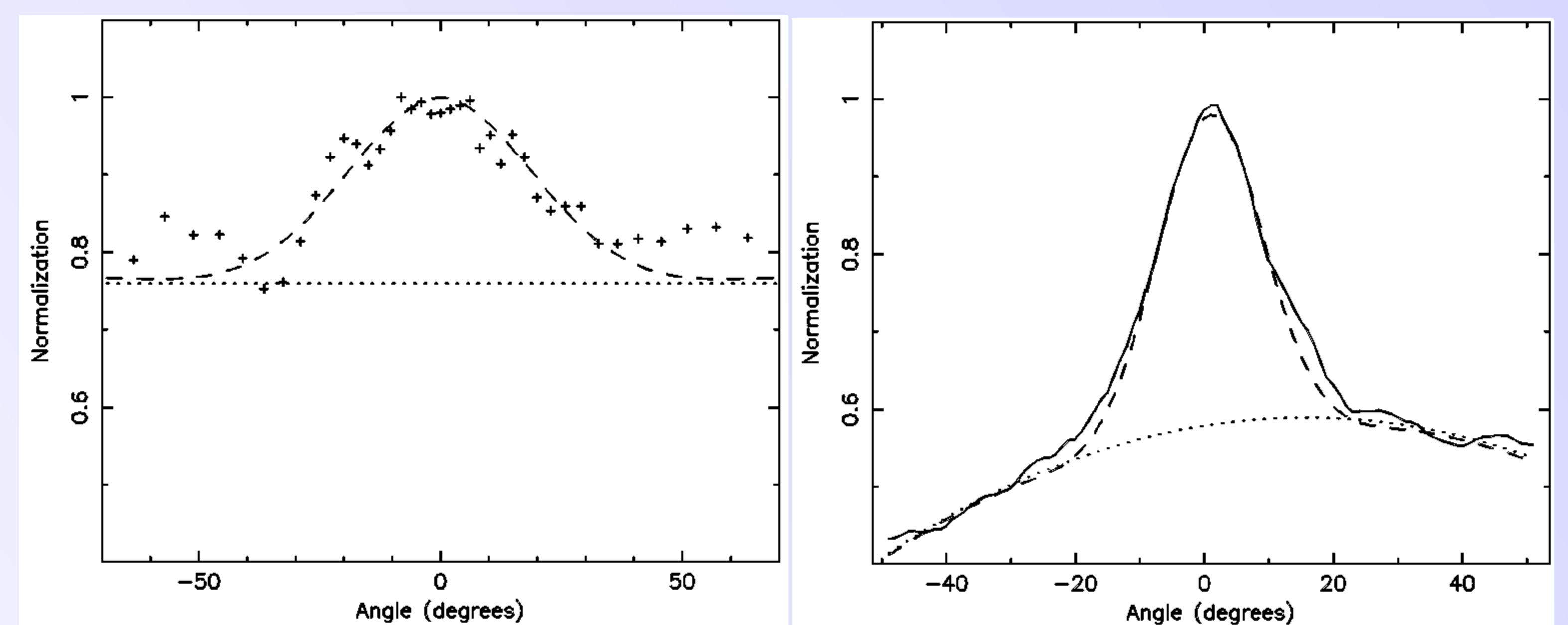


Figure 4. Left: Two year average azimuthal X-ray intensity distribution in an elliptical annulus at distance of 8'' to the northwest of the pulsar. Right: The average azimuthal distribution of the optical data nearest the pulsar. **Note the different widths implying significantly different Doppler boosting factors** with the optical more strongly boosted than the X-ray in contradiction with the results of global numerical MHD modeling (e.g. Komissarov & Lyubarsky 2003; Bucciantini et al. 2005).

## References

- Bietenholz M. F., Hester J. J., Frail D. A., Bartel N., 2004, ApJ, 615, 79
- Bucciantini N., del Zanna L., Amato E., Volpi D., 2005, A&A, 443, 519
- Komissarov S. S., Lyubarsky Y. E., 2003, MNRAS, 344, L93